

Image reconstruction
using parallel Monte Carlo simulations

Ryoichi Mizuno *
Department of Physics, Sophia University

February 22, 2001

Contents

1	Model and formulation	3
1.1	Image reconstruction formulation	3
1.2	Reconstruction temperature	5
2	Methods of simulations	6
2.1	Monte Carlo method	6
2.2	Message passing interface	7
2.3	Sub-lattice method	7
3	Simulations	8
3.1	Image reconstruction	8
3.2	Reconstruction of photographs	10
3.3	Reconstruction temperature	11
3.4	Boundary condition effect	13
3.5	Effect of parallelization by MPI	14

Abstract

In the mathematical engineering fields, reconstruction of damaged images that were damaged by data transmission through a channel (e.g. sent by a defective fax, a fickle e-mail, etc.) has been regarded as a sort of optimization problems. On the other hand, from the view point of the statistical mechanics, it is regarded as determining the state of equilibrium of the random spin system. This is readily achievable by a priori knowledge that generally, an image does not alter abruptly. By regarding a pixel to spin and by introducing Hamiltonian the energy of which gets lower when neighboring sites were the same spin, image reconstruction is reduced to obtain the thermal equilibrium of spin system.

In this report, the validity of image reconstruction by the methods of the statistical mechanics is verified.

MPI (Message Passing Interface) library implementation for parallel computation is used, which shortens the time of simulations.

1 Model and formulation

1.1 Image reconstruction formulation

In this paper, reconstruction of damaged monochrome binary images is studied. An image is described as the Ising spins $\{\xi_i\}$, where i is pixel number that corresponds to site number in the spin system.

Information of the original image $\{\xi_i\}$ is damaged by a channel. Received information of the pixel i , τ_i , is damaged with probability p , and turned into reverse of ξ_i . The channel gives noise each site independently, and the probability that a white pixel is turned into a black one and that of reversing are the same (memoryless binary symmetric channel).

The output function of the channel for the pixel i is thus given by the conditional probability

$$P_{\text{out}}(\tau_i | \xi_i) = \frac{\exp(\beta_p \tau_i \xi_i)}{2 \cosh \beta_p}, \quad (1)$$

$$\exp(2\beta_p) \equiv \frac{1-p}{p}. \quad (2)$$

Under the assumption of independent noise at each pixel, the output function for the whole image is the product of equation (1):

$$P_{\text{out}}(\{\tau\} | \{\xi\}) = \frac{1}{(2 \cosh \beta_p)^N} \exp\left(\beta_p \sum_i \tau_i \xi_i\right), \quad (3)$$

where N is the total number of pixels of the image.

The desired conditional probability (the posterior) that is the function $P(\{\xi\} | \{\tau\})$ is obtained by the Bayes formula (equation 8). This is necessary to estimate the original image $\{\xi\}$ from the damaged image $\{\tau\}$.

The estimated image is defined as $\{\sigma\}$ to distinguish the reconstructed image

from the original image.

From the Bayes formula, posterior is given by

$$P(\{\sigma\} | \{\tau\}) = \frac{\exp\left(\beta_p \sum_i \tau_i \sigma_i\right) P_s(\{\sigma\})}{\text{Tr}_\sigma \exp\left(\beta_p \sum_i \tau_i \sigma_i\right) P_s(\{\sigma\})}, \quad (4)$$

where $P_s(\{\sigma\})$ is the generation probability of the original image (the prior). The prior $P_s(\{\sigma\})$ expresses how the original image was made. Generally, one does not know the correct prior $P_s(\{\sigma\})$.

Therefore, I introduced a model prior:

$$P_m(\{\sigma\}) \equiv \frac{\exp\left(\beta_m \sum_{(ij)} \sigma_i \sigma_j\right)}{Z(\beta_m)}, \quad (5)$$

where (ij) runs over neighboring pixels, $Z(\beta_m)$ is the partition function of the ferromagnetic Ising model at temperature $T_m (= \beta_m^{-1})$ and β_m is the parameter of how smooth the original image is. This is based on the priori knowledge of image that generally, the pixel of image does not alter abruptly.

Thus,

$$P(\{\sigma\} | \{\tau\}) = \frac{\exp\left(\beta_p \sum_i \tau_i \sigma_i + \beta_m \sum_{(ij)} \sigma_i \sigma_j\right)}{\text{Tr}_\sigma \exp\left(\beta_p \sum_i \tau_i \sigma_i + \beta_m \sum_{(ij)} \sigma_i \sigma_j\right)} \quad (6)$$

is given by equation (4) and (5). This is the posterior of the estimated image $\{\sigma\}$ when the damaged image $\{\tau\}$ is given. The most probable $\{\sigma\}$ is the $\{\sigma\}$ that maximize the posterior.

In terms of the spin system, maximization the posterior equivalent to maximization the Boltzmann factor of the ferromagnetic Ising model in the presence of random magnetic fields.

Therefore, the image reconstruction Hamiltonian:

$$H = - \left(\frac{\beta_p}{\beta_m} \sum_i \tau_i \sigma_i + \sum_{(ij)} \sigma_i \sigma_j \right) \quad (7)$$

is introduced. The original image reconstruction problem is reduced to maximizing the free energy of the above random magnetic field Ising model.

The Bayes formula:

Generally, when there are two events A and B , the probability that both of events occur $P(A, B)$ is given with the conditional probability that event A occurs under a condition that event B occurred $P(A | B)$ and the conditional probability that event B occurs under a condition that event A occurred $P(B | A)$.

Equation these leads to

$$P(A, B) = P(A | B) P(B) = P(B | A) P(A).$$

Thus,

$$P(A | B) = \frac{P(B | A) P(A)}{P(B)} = \frac{P(B | A) P(A)}{\sum_A P(B | A) P(A)} \quad (8)$$

is proven.

1.2 Reconstruction temperature

Generally, one does not know the degree of damage. Therefore, I replace β_p to a general variable h in the later argument. The prior $P_s(\{\xi\})$ is now assumed to be given by

$$P_s(\{\xi\}) = \frac{\exp\left(\beta_s \sum_{(ij)} \xi_i \xi_j\right)}{Z(\beta_s)}, \quad (9)$$

where β_s is the inverse of temperature when the original image was generated. The product of the pixel of the original image ξ_i and the corresponding pixel of the estimated image σ_i is $+1$ for $\xi_i = \sigma_i$ and -1 for $\xi_i \neq \sigma_i$. The average over the sum of all of the products by the output function of the channel $P_{\text{out}}(\{\tau\} | \{\xi\})$ (equation 3) and the prior $P_s(\{\xi\})$ (equation 9) is defined as the overlap:

$$\begin{aligned} M(\beta_m, h) &= \text{Tr}_\xi \text{Tr}_\tau P_s(\{\xi\}) P_{\text{out}}(\{\tau\} | \{\xi\}) \xi_i \text{sgn}\langle\sigma_i\rangle \\ &= \frac{1}{(2 \cosh \beta_p)^N Z(\beta_s)} \text{Tr}_\xi \text{Tr}_\tau \exp\left(\beta_p \sum_i \tau_i \xi_i + \beta_s \sum_{(ij)} \xi_i \xi_j\right) \xi_i \\ &\quad \times \text{sgn}\langle\sigma_i\rangle, \end{aligned} \quad (10)$$

where Tr_ξ and Tr_τ mean the sum over $\{\xi\}$ and that over, respectively $\{\tau\}$, and $\langle\sigma_i\rangle$ means the average by the Boltzmann factor in the right hand side of equation (6) β_p being replaced by h .

The absolute value of the overlap satisfies

$$\begin{aligned}
& M(\beta_m, h) \\
& \leq \frac{1}{(2 \cosh \beta_p)^N Z(\beta_s)} \left| \text{Tr}_\xi \text{Tr}_\tau \exp \left(\beta_p \sum_i \tau_i \xi_i + \beta_s \sum_{(ij)} \xi_i \xi_j \right) \xi_i \right| \\
& = \frac{1}{(2 \cosh \beta_p)^N Z(\beta_s)} \frac{\left\{ \text{Tr}_\xi \text{Tr}_\tau \exp \left(\beta_p \sum_i \tau_i \xi_i + \beta_s \sum_{(ij)} \xi_i \xi_j \right) \xi_i \right\}^2}{\left| \text{Tr}_\xi \text{Tr}_\tau \exp \left(\beta_p \sum_i \tau_i \xi_i + \beta_s \sum_{(ij)} \xi_i \xi_j \right) \xi_i \right|} \\
& = \frac{1}{(2 \cosh \beta_p)^N Z(\beta_s)} \text{Tr}_\xi \text{Tr}_\tau \exp \left(\beta_p \sum_i \tau_i \xi_i + \beta_s \sum_{(ij)} \xi_i \xi_j \right) \xi_i \\
& \quad \times \frac{\text{Tr}_\xi \text{Tr}_\tau \exp \left(\beta_p \sum_i \tau_i \xi_i + \beta_s \sum_{(ij)} \xi_i \xi_j \right) \xi_i}{\left| \text{Tr}_\xi \text{Tr}_\tau \exp \left(\beta_p \sum_i \tau_i \xi_i + \beta_s \sum_{(ij)} \xi_i \xi_j \right) \xi_i \right|} \\
& = \frac{1}{(2 \cosh \beta_p)^N Z(\beta_s)} \text{Tr}_\xi \text{Tr}_\tau \exp \left(\beta_p \sum_i \tau_i \xi_i + \beta_s \sum_{(ij)} \xi_i \xi_j \right) \xi_i \\
& \quad \times \text{sgn}(\sigma_i)_{\beta_s, \beta_p} \\
& = M(\beta_s, \beta_p), \tag{11}
\end{aligned}$$

where $\text{sgn}(\sigma_i)_{\beta_s, \beta_p}$ means the average by the Boltzmann factors. Therefore, the inequality

$$M(\beta_m, h) \leq M(\beta_s, \beta_p) \tag{12}$$

is obtained.

The overlap is the parameter of how good the reconstruction is, and it takes its maximum when $\beta_m = \beta_s$ and $h = \beta_p$. Note that the most optimized reconstruction is realized at finite temperature ($\beta_m^{-1} \neq 0$ and $h^{-1} \neq 0$).

The inequality (12) was proved under the condition that the original image is generated by the Boltzmann factor of the ferromagnetic Ising model. However, even when the original image is a natural image, the most optimized reconstruction is also realized at finite temperature.

In this study, using a fixed value of $\beta_p = h$, β_m is changed.

2 Methods of simulations

2.1 Monte Carlo method

Monte Carlo method is a stochastic technique that is used in many fields of sciences, ranging economics, nuclear physics to regulating the flow of traffic.

Metropolis algorithm, which is a very efficient way to determine the thermal equilibrium, is described as follows:

At first, a spin of a site is reversed. Then, the difference between energy of the system before and after the reverse of the spin ΔE is calculated. If energy difference $\Delta E \leq 0$, the reverse of the spin is accepted. On the other hand, if $\Delta E > 0$, the reverse of the spin is accepted with the probability $e^{-\beta_m \Delta E}$. This operation is applied to every spin. After sufficient iteration, the state of thermal equilibrium is reached.

This is understood as follows:

From the detailed balance,

$$P(\nu | \mu) P(\mu) = P(\mu | \nu) P(\nu) \quad (13)$$

should be satisfied, where μ and ν are the spin states.

From this equation, the probability of reversing spin becomes

$$\frac{P(\mu | \nu)}{P(\nu | \mu)} = \frac{P(\mu)}{P(\nu)} = e^{-\beta(E_\mu - E_\nu)} \equiv e^{-\beta_m \Delta E}. \quad (14)$$

$$(15)$$

In this study, the probability that higher energy state turns into lower energy state by reversing of spin $P(\nu | \mu)$ is defined as 1. Therefore, the probability that higher energy state turns into lower energy state by reversing of spin $P(\mu | \nu)$ is given by

$$P(\mu | \nu) = e^{-\beta_m \Delta E}. \quad (16)$$

2.2 Message passing interface

MPI stands for Message Passing Interface that is a widely used standard library for implementing parallel programs using message passing. MPI is easy, highly efficient and flexible.

Recently, it is proved that the message passing system is effective and simple implementation for some systems.

In this study, plenty of simple same computation is needed for the each pixel, but the necessary information is only the information of the neighboring pixels. Therefore, I introduced MPI to proceed simulations on separate process.

2.3 Sub-lattice method

To introduce MPI library implementation for parallelization, I divided the images equally (see the left of figure 1). The each piece of the image is simulated on separate process.

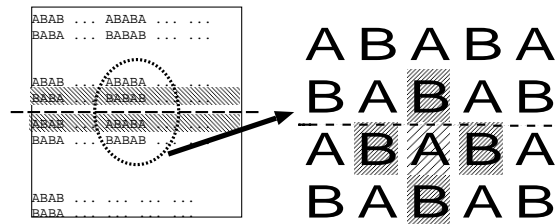


Figure 1: sub lattice method

In Figure 1, I showed the case of 2 processes.

At the border (see shaded part of the left of figure 1), lack of information of the neighboring pixels is occurred. Then, every sweeping of the image, the each process sends and receives their information each other by message passing. In this case, some pixels use old information of the neighboring pixels. To overcome this difficulty, I defined pixels as sub-lattice *A* and sub-lattice *B* alternately. First, the pixels sub-lattice *A* are swept. Then, the pixels the sub-lattice *B* are swept. As the result of this operation, the neighboring pixels of the object pixel are always on the different sub-lattice.

3 Simulations

3.1 Image reconstruction

I used two dual Intel® Pentium® III Processor 800 MHz CPU machines for simulations of this study. Each machine is connected by 100 Mbps LAN. I made parallel program for simulations in C language with MPI library implementation.

I introduced a 256×256 monochrome binary image of the outline of Dæmon¹ (figure 2) for the original image.



Figure 2: original image (Dæmon)

¹the mascot character of FreeBSD

And, I generated the 10% damaged image (figure 3) and the 20% damaged image (figure 4) of the original image. Then, I performed simulations for the reconstruction of the damaged images described above (figure 3 and 4).



Figure 3: 10% damaged image of Figure 2

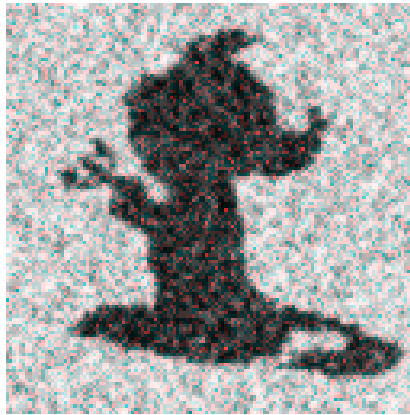


Figure 4: 20% damaged image of Figure 2

The reconstructed images (figure 5 and 6) reproduce the original image well.



Figure 5: reconstructed image of Figure 3



Figure 6: reconstructed image of Figure 4

3.2 Reconstruction of photographs

Simple images such as figure 2 satisfies the assumption of this study that is “Generally, if there is an isolated white (or black) site on black (or white) background, the possibility that it is noise is high.”

However, more complex images such as an image that is generated from a photograph such as figure 7 do not satisfy the assumption in general.



Figure 7: original image that was generated from a photograph (Boltzmann)

In this case, bright and dark part of the image is expressed as density of the white pixels and the black pixels. So, it is impossible to distinguish noise from the parts where the white pixels and black pixels are distributed with the almost same probability. Therefore, the more complex images such as an image that is generated from a photograph can not be reconstructed well (see figure 8).



Figure 8: reconstructed image of 10 % damaged image of Figure 7

3.3 Reconstruction temperature

I determined β_m that realized the optimized reconstructions by changing β_m of figure 2 and 7. The most optimized reconstructions is realized at finite temperature (see figure 9 and 10).

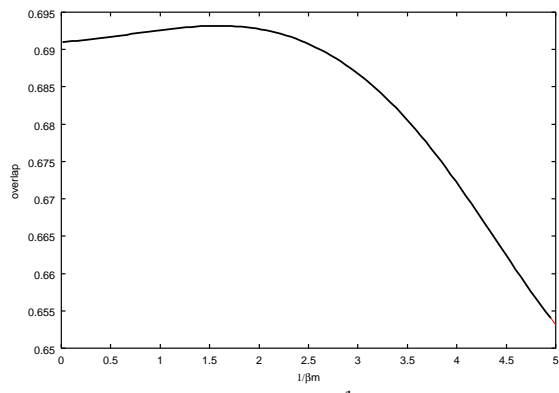


Figure 9: overlap and $\frac{1}{\beta_m}$ of Figure 5

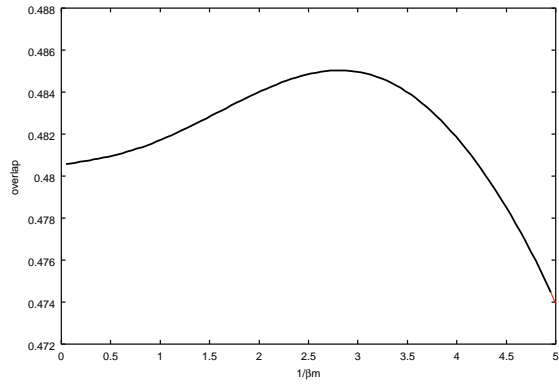


Figure 10: overlap and $\frac{1}{\beta_m}$ of Figure 8

When the absolute zero of temperature is assumed, details of the image are not reproduced well (see figure 11).



Figure 11: reconstructed image of figure 3 at absolute 0 degree

3.4 Boundary condition effect

In this study, I introduced the free boundary condition that 0 spins are put around the image. This condition reduces the interactions of the spins of the edge of the image. This is based on a priori knowledge that generally, the top and the bottom (or the left edge and the right edge) of image do not have a mutual relation.

On the other hand, the most common boundary condition of simulations of studies of the statistical mechanics is the periodic boundary condition. However, if the periodic boundary condition is introduced for boundary condition of this study, sometimes unexpected white (or black) pixels appear in the reconstructed image.

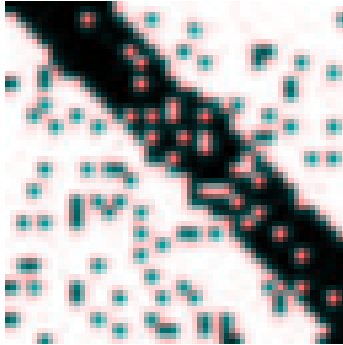


Figure 12: damaged image (slash)



Figure 13: reconstructed image of figure 12 by the periodic boundary condition

At the right upper part of figure 13, unexpected black pixels appeared. Due to the introduction of the periodic boundary condition, at the right upper part of the damaged image (figure 12), the state of high distribution of black pixels occurs.

However, for seamless images, the periodic boundary condition is better than the free boundary condition.

3.5 Effect of parallelization by MPI

In this study, I equally divided the images into 4 pieces (see figure 14) to introduce MPI library implementation.



Figure 14: divide an image

As the result of the introduction of MPI library implementation, efficiency got better (see figure 15).

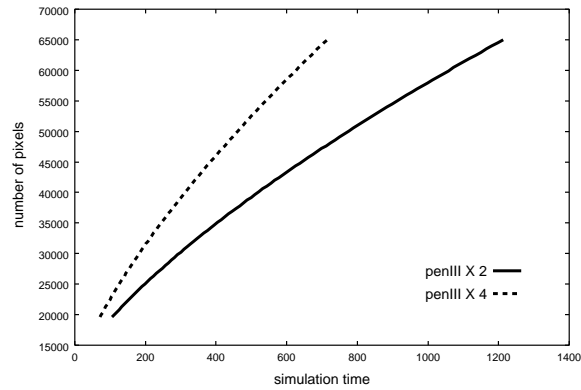


Figure 15: efficiency of MPI

The abscissa of figure 15 is the time of the simulations and the vertical line is the number of the pixels. In this study, number of the sweeping is proportional to the number of the pixels. Therefore, the vertical line is number of the sweeping. In the large number pixels region, the simulation time is almost proportional to number of CPU. On the other hand, the simulation time is not proportional to number of CPU when number of pixels is small. Because, message passing

needs longer time than communication between CPU, memory, and cache. This fact shows that introduction of MPI library implementation is efficient if the image to be reconstructed is sufficiently large.

Summary

In this thesis, validity of image reconstruction of simple images such as figure 2 by the methods of the statistical mechanics is demonstrated.

However, image reconstruction of more complex images such as an image that is generated from a photograph is not achieved. To treat more complex images, another model such as Potts model may be necessary, which is left for the future.